Biaxial low-cycle fatigue failure of TYPE 304 stainless steel under in-phase and out-of-phase straining conditions

Takashi Ogata, Akito Nitta and Kazuo Kuwabara
Central Research Institute of Electric Power Industry,
Tokyo, Japan

Third International Conference on Biaxial/Multiaxial Fatigue,
April 3-6, 1989 Stuttgart, FRG

ABSTRACT

Axial-torsional strain-controlled fatigue tests of TYPE 304 stainless steel were conducted under in-phase and out-of-phase straining conditions, at room temperature and 650°C. As a result, the fatigue life under the out-of-phase straining condition was found to be shorter than under the in-phase condition in the same applied strain range at both testing temperatures. The observation of fracture surface and microcracks on the fracture surface indicated that this descrepancy in fatigue life should be due to difference in the fracture mode related to the macroscopic strain condition between the in-phase and out-of-phase straining. Biaxial fatigue life could not be evaluated successfully by clsssical criteria, so that the new criterion applied to the out-of phase straining condition was proposed by modifying the Γ-plane theory proposed by Brown and Miller. Consequently, biaxial fatigue life could be correlated well with the equivalent shear strain range independent of the straining condition.

INTRODUCTION

The majority of mechanical components and structures in service are generally subjected to biaxial/multiaxial cyclic loading condtions. Particularly complex multiaxial loading conditions, such as out-of-phase or nonproportional loading, due to the interaction of mechanical and theraml cyclic stresses are resulted in elevated temperature structures such as fast breeder reactor vessels and pipings. Under such loading conditions the principal stress and strain axes rotate during fatigue loading. Therefore design of component has to be done based on the accurate criterion which can evaluate fatigue life under proportional and nonproportional loading conditions.

In the present design procedure, multiaxial stress or strain conditions are reduced to an equivalent uniaxial condition based on the classical yield criteria such as Tresca or von Mises theory and fatigue strength is estimated from laboratory uniaxial fatigue data. In a recent multiaxial fatigue study, however, it has been reported that these classical criteria are not always effective in predicting low-cycle fatigue (LCF) life under multi-axial fatigue conditons (1-3). In the biaxial LCF region, various criteria have been proposed and their validity discussed (4-7). The critical plane approach proposed by Brown and Miller (4) which is one of the new criteria taken into account for the behaviour of crack initiation and propagation, is widely studied for correlating multiaxial fatigue data at room and elevated temperatures (2, 8-10). Brown and Miller (4) suggested that the maximum shear strain γ_{max} and normal strain ε_n on the γ_{max} plane are the important parameters governing fatigue life. Kadil, Brown and Miller (9) defined equivalent shear strain which contains two critical strains and has obtained good evaluation results of biaxial fatigue data for AISI 316 stainless steel. Blass and Zamrik (2) conducted a tension-torsion test on AISI 304 stainless steel and reported that the critical plane approach would be more effective than criteria based on classical equi-valent strains. Socie et al. (10) also reported that the biaxial fatigue life of IN 718 was correlated well with equivalent shear strain parameter incorporating mean stress term.

However, most of the previous studies have been conducted under proportional loading conditions, while the experimental results obtained under nonproportional loading are very few (10-13). The authors (14, 15) have investigated biaxial LCF behaviour of TYPE 304 stainless steel at 550°C by conducting axial-torsional fatigue tests under proportional and nonpro-portional loading conditions, and have suggested that new criteria derived from the critical plane approach extending in the nonproportional region could evaluate biaxial fatigue life well, independently of the proportional and nonproportional loading conditions.

In this study, axial-torsional fatigue tests of TYPE 304 stainless steel were conducted under in-phase and out-of-phase conditions at room temperature and at 650°C. The fracture mode and low cycle fatigue criterion were discussed based on the results obtained at both temperatures along with the results obtained previously at 550°C.

EXPERIMENTAL PROCEDURE

Specimen and test equipment

The material used in this study is TYPE 304 stainless steel, solution treatment at 1050°C for 10 min in vacuume followed by water cooling. The chemical composition is as follows : 0.05C, 0.47Si, 0.83Mn, 0.03P, 0.009S, 9.11Ni and 18.63Cr. A thin-walled cylindrical specimen with an outside diameter of 13mm and a thickness of 1.5mm is shown in Fig. 1. The inside surface had been lapped and the outer surface had been finished with emery paper through grade No. 1000, then polished lightly with alumina powder. The equipment used for the test was a computer-controlled electrohydraulic servo-driven push-pull and torsional fatigue machine incorporated with an induction heater. Strain within a gauge length of 12.5mm was measured with a high-temperature biaxial extensometer which permitted the separate measurement of axial and torsional strains.

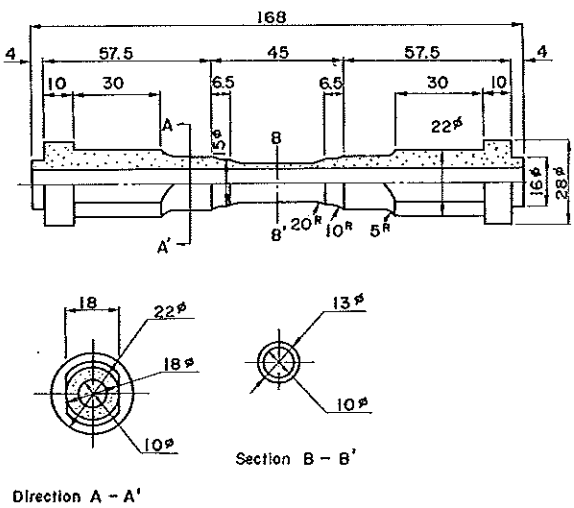

Fig. 1 Specimen geometry.

Test conditions

Axial-torsional strain-controlled LCF tests were carried out at R.T. and 650°C under two different sinusoidal straining conditions. One is in-phase or proportional straining and the other is out-of-phase (90° phase difference between the axial and torsional strains) or nonproportional straining. A strain ratio, φ, was defined as the ratio of the torsional strain range, $\Delta\gamma$, to the axial strain range, $\Delta\varepsilon$, (i.e., $\varphi=\Delta\gamma/\Delta\varepsilon$). For the in-phase tests the Mises equivalent strain range was selected from 0.7 to 1.4% with a cycle period of 14 to 28 seconds where the creep effect could be neglected at 650°C. The same cycle period and values of $\Delta\gamma$ and $\Delta\varepsilon$ were used for the out-of-phase tests. All test conditions are shown in Table 1 together with test results. Fatigue failure life was defined as the number of cycles that resulted in a 25% drop from the maximum value in either tensile stress or shear stress. The main crack length on the failure specimen was about 10 to 15mm. The fracture surface of a failed specimen was observed with a scanning electron microscope (SEM).

The detail of the strain condition under in-phase and out-of-phase straining has already been reported (15). In order to easily understand the relationship between the strain condition and the fracture modes, only the results of strain analysis are shown here. Fig. 2 shows the variation in $\Delta\varepsilon_\theta$ and under in-phase and out-of-phase straining conditions, where and $\Delta\gamma_\theta$ are the normal and shear strain range during one cycle in a direction inclined at an arbitrary angle θ to the specimen axis. In the in-phase case the maximum principal strain direction is displaced 45deg. from the maximum shear strain direction whilst the $\Delta\gamma_\theta$ in the out-of-phase straining is nearly equal to its maximum value in all directions and both the maximum $\Delta\varepsilon_\theta$ and $\Delta\gamma_\theta$ occur on the same plane or normal to the specimen axis.

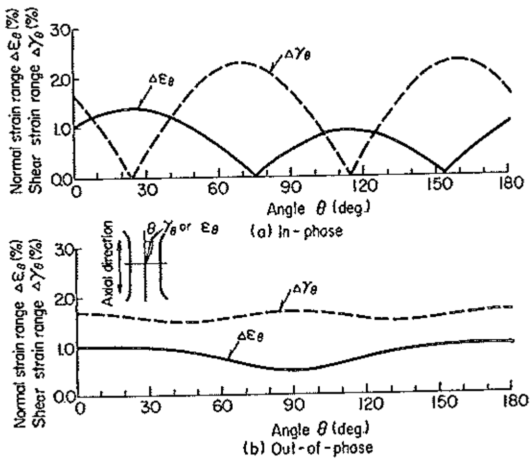

Fig. 2 Normal and shear strain states in in-phase and out-of-phase tests.

RESULTS AND DISCUSSION

Fracture mode under biaxial loading condition

Typical examples of failed specimens under in-phase condition at R.T. and 650°C are shown in Fig. 3. In the following

Table 1 Test conditions and results

a) Room Temperature

	Specimen number	Strain ratio	Axial strain range $\Delta\varepsilon$ (%)	Torsional strain range $\Delta\gamma$ (%)	at 1/2 Nf data Axial stress range $\Delta\sigma$ (MPa)	Torsional stress range $\Delta\tau$ (MPa)	Number of cycles to failure Nf (Cycles)
In-phase	IN1-1	0	1.4	0	611	0	3080
	IN1-2		0.7	0	438	0	16000
	IN1-3	1.7	1.0	1.7	452	267	4300
	IN1-4		0.71	1.21	394	224	10834
	IN1-5		0.5	0.85	325	204	26300
	IN1-6	∞	0	2.43	0	385	10970
	IN1-7		0	1.21	0	256	48300
Out-of-phase	OU1-1	1.7	0.71	1.21	903	413	3150
	OU1-2		0.5	0.85	704	321	9530
	OU1-3	3.67	0.43	1.58	657	387	4500
	OU1-4		0.3	1.1	546	356	11800

b) 650°C

	Specimen number	Strain ratio	Axial strain range $\Delta\varepsilon$ (%)	Torsional strain range $\Delta\gamma$ (%)	at 1/2 Nf data Axial stress range $\Delta\sigma$ (MPa)	Torsional stress range $\Delta\tau$ (MPa)	Number of cycles to failure Nf (Cycles)
In-phase	IN2-1	0	1.4	0	500	0	510
	IN2-2		1.0	0	442	0	880
	IN2-3		1.0	0	450	0	980
	IN2-4		0.7	0	393	0	3370
	IN2-5		0.7	0	394	0	3710
	IN2-6	1.7	1.0	1.7	409	192	530
	IN2-7		0.71	1.21	346	166	1720
	IN2-8		0.5	0.85	328	160	4400
	IN2-9	3.67	0.6	2.2	301	238	560
	IN2-10		0.43	1.57	263	221	1720
	IN2-11		0.3	1.1	232	198	4120
	IN2-12	∞	0	2.43	0	267	730
	IN2-13		0	1.73	0	245	2740
	IN2-14		0	1.21	0	211	7980
Out-of-phase	OU2-1	1.7	0.71	1.21	553	313	440
	OU2-2		0.5	0.85	482	268	1330
	OU2-3		0.36	0.61	394	227	4960
	OU2-4		0.36	0.61	405	219	4350
	OU2-5	3.67	0.6	2.2	532	312	250
	OU2-6		0.43	1.57	484	293	710
	OU2-7		0.3	1.1	394	252	2100

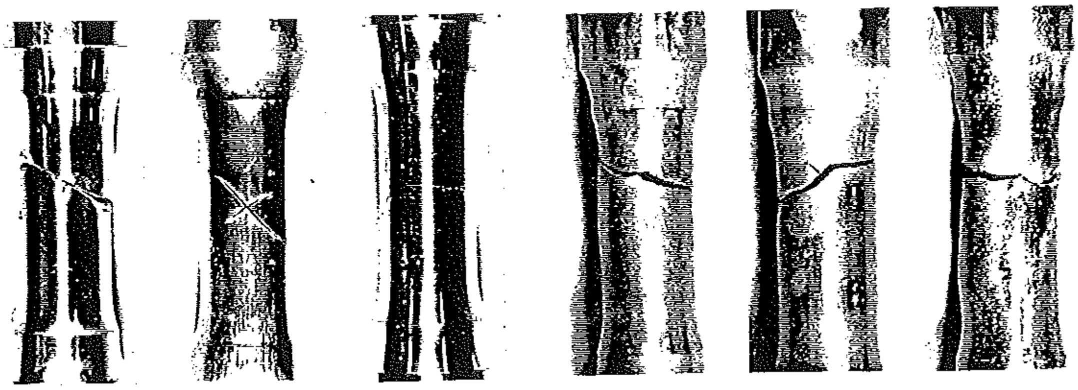

φ=1.7(IN) $\varphi=\infty$ φ=1.7(OUT) φ=1.7(IN) $\varphi=\infty$ φ=1.7(OUT)

a) R.T. b) 650°C

Fig. 3 Fracture appearance of failed specimens.

discussion the term "Mode I" refers to the case where the main crack propagated in the direction normal to the ε, direction and the term "Mode II" refers to the case where the main crack propagated in the γ_{max} plane. The main cracks of all specimens at room temperature propagated in the Mode I fracture direction independently of strain ratios and strain ranges. From the observation of surfaces on failed specimens, it was found that microcracks of about 0.1mm in length initiated from the grain-boundary normal to the direction, but the nucleation density of microcracks is lower than that at 650°C and this indicates that a failure occured by the propagation of a single main crack. Socie et al. (10) also observed the fracture surfaces of the AISI TYPE 304 stainless steel after tension-torsion tests and reported that the majority of the life was consumed in Mode I growth under tension and torsion in-phase loading. On the other hand the Mode I fracture occured at φ=0, 1.7, 3,67 and ∞ ($\Delta\gamma \geq 1.73\%$) and the Mode I fracture occured at $\varphi=\infty$($\Delta\gamma$=1.21) at 650°C. The examination of specimen surfaces tested in in-phase straining indicated that most of the microcracks initiated from the oxide layer, which were formed partly on a specimen surface, in a direction normal to the ε_1 direction. These microcracks then propagated to form macrocracks or the main crack along the same direction at φ=0, 1.7, 3.67. For a Mode II fracture specimen in torsion, on the other hand, microcracks oriented at 45° with respect to the specimen axis and propagated, eventually link to form macrocracks γ_{max} plane. The microcracks of the specimen, which showed Mode I fracture macroscopically, propagated in the γ_{max} plane until becoming about 1mm in length. Furthermore all of the microcracks initiated outside of the oxide layer and then propagated in the γ_{max} plane. Sakane et al. (16) conducted the detailed observation of micro- and macrocrack formations on the specimens tested under in-phase tension-torsion condition at 650°C, and indicated that although the failure modes of macrocracks shifted from Mode I to Mode II at $\varphi=3.0$, microcracks initiated in a direction normal to the ε_1 direction at all strain ratios because the surface oxide layer was the cause of opening type (i.e., Mode I) microcrack.

As previously reported, a crack initiation occured on the γ_{max} plane under all in-phase tests at 550°C and the fracture mode was distinctly classified into either Mode I or II, and the transition point occured in the vicinity of the strain ratio of 1.7. Microcrack formations and fracture modes at R.T., 550°C and 650°C are summarized in Table 2. At each temperature,

Table 2 Microcrack direction and failure mode.

Temperature	Microcrack direction	Failure mode of macrocrack
B.T.	Normal to the ε_1 direction	Mode I ...$\varphi=0 \sim \infty$
550°C	Parallel to the γ_{max} plane	Mode I ...$\varphi\leq 1.7$ Mode II ..$\varphi>1.7$
650°C	. In oxide layer Normal to the direction . Outside of oxide layer Parallel to the γ_{max} plane	Mode I ...$\varphi=0,1.7,3.67$ $\infty(\Delta\gamma\geq 1.73\%)$ Mode II...$\varphi=\infty(\Delta\gamma=1.21\%)$

microcracks of a few grain size start from the grainboundary except for the ones in the oxide layer at 650°C. Most of the grainboundary microcracks at R.T. create in a direction normal to the ε_1 direction, while most of the grainboundary microcracks at 550°C and 650°C are on the γ_{max} plane. This descrepancy may be attributed to the grainboundary sliding oriented to the γ_{max} direction, and occurs easily at elevated temperatures as compared to the behaviour at R.T.. The transition condition of fracture mode varys with the test temperature and the applied strain range due to high temperature oxidation and the microscopic stress and strain states at a region ahead of a crack. Currently the continuous observation of the fatigue process under in-phase and out-of-phase biaxial fatigue conditions at both room and elevated temperatures are being conducted, in order to investigate the crack initiation and propagation behaviours.

The typical fracture appearance of the specimens tested under out-of-phase condition at R.T. and 650°C are shown in Fig. 3. The main cracks in most of the specimens propagated on the circumferential direction where the peak value of both normal strain and shear strain occured as shown in Fig. 2 (b). Microcracks around the macrocrack also propagated in the circumferential direction at both temperatures. The fracture mode is obviously different from that in the in-phase condition at the same strain ratio. In most of the specimens tested under out-of-phase condition, microcrack initiation occured in the plane of the maximum shear strain range and then propagated to form a maincrack in the same plane.

Failed specimens were examined by SEM. Typical examples of the specimen surface in in-phase and out-of-phase tests at 650°C are shown in Fig. 4. Striations were observed on the fracture surfaces of specimens that failed in Mode I at both temperatures, while rub mark caused by contact of fracture surfaces was observed on specimens that failed in Mode II. In the out-of-phase condition, on the other hand, both striations and rub

$\varphi=1.7$(IN) $\varphi=\infty$ $\varphi=1.7$(OUT)

Fig. 4 Typical fracture surface of failed specimen at 650° C marks were observed on the fracture surface, and it indicated that the maincrack propagated under a mixed mode combining Mode I and II. It seems that a mixed mode fracture owing to the maximum shear strain and the maximum normal strain with the 90° phase difference in the crack propagation plane resulted in a shorter fatigue life in out-of-phase conditions than that in in-phase conditions at the same applied strain.

Biaxial fatigue failure criterion

As mentioned above, the fracture mode under biaxial loading conditions varys, with the test temperature and the applied strain range. Therefore, if a fracture mode in one test condition is different from that in another one, it is appropriate to apply different fatigue failure criteria, which are based on a reasonable physical interpretation, to fatigue life evaluation under each condition. From this point of view, the authors (15) have been investigating the critical plane approach and the energy based approach which could be taken into account for the fracture mode differences. As a result, it was indicated that each criterion could be correlated well with biaxial LCF data at 550°C. However, since a fracture mode can not be always provided in a design of actual components and structures, a criterion which can evaluate the fatigue life is desirable when fracture mode cannot be identified. At present the Mises equivalent strain is applied to the design criteria of high temperature structure, such as ASME CODE CASE N-47. Biaxial LCF data under in-phase and out-of-phase conditions at R.T. and 650°C correlated with the Mises equivalent strain range are shown in Fig. 5. At both temperatures there is a tendency for fatigue life to depend

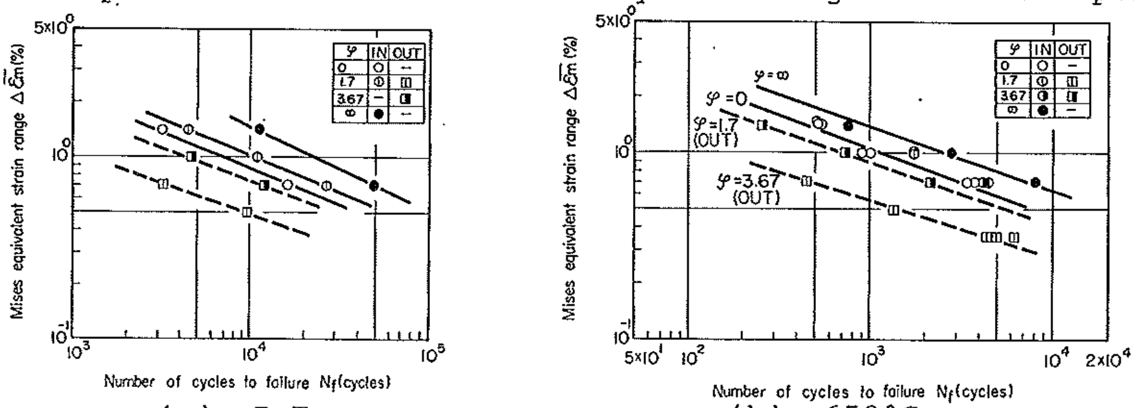

(a) R.T. (b) 650°C

Fig. 5 Correlation of biaxial LCF data with Mises equivalent strain range.

on the strain ratio, with uniaxial fatigue giving the shortest life among in-phase data. Furthermore fatigue life under out-of-phase condition was found to be from one half to one quarter shorter than that in uniaxial fatigue. The same tendency was seen in the Tresca criterion. From these findings, the same as at 550°C (14, 15), it is seen that the classical theories are not applicable as a biaxial LCF criterion. In order to evaluate the biaxial LCF life independently of in-phase and out-of-phase loading conditions, the authors have extended the Γ-plane theory to an out-of-phase region based on the fractographic observation and strain analysis results.

In this paper, the biaxial LCF criterion was derived from the modified Γ-plane for biaxial LCF data at R.T., 550°C and 650°C, and the temperature dependency of experimental constants in the criterion was discussed. Then the criterion was verified from its applicability to correlate with the biaxial LCF data obtained by other researchers.

The authors (15) have obtained a lot of biaxial LCF data at 550°C under in-phase conditions (φ=0, 1.5, 1.7, 2.5, 3.67, ∞) as well as under out-of-phase conditions (φ=1.5, 1.7, 2.5, 3.67, 8) at λ (phase difference) =90° and φ=1.5 at λ=30°, 45°, 60°). Based on these results iso-Nf contours were constructed on the $\Delta\gamma_{max}/2-\Delta\varepsilon_n$ plane (called

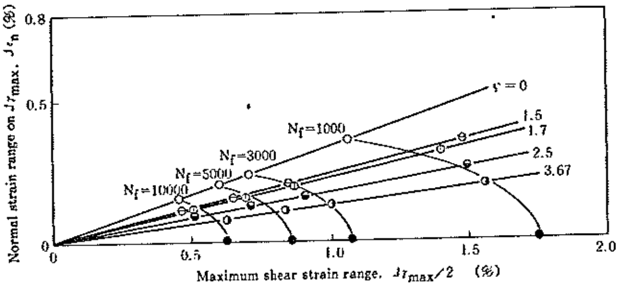

(a) In-phase

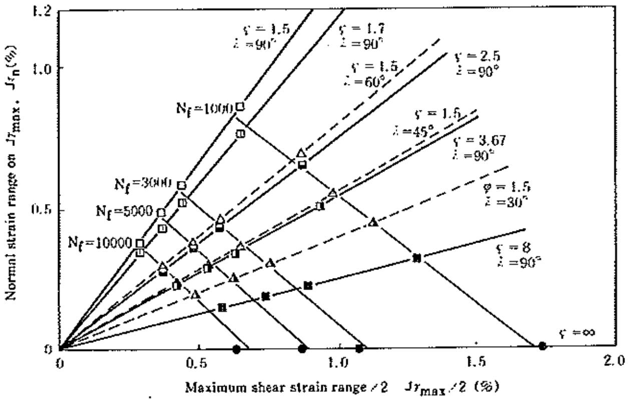

(b) Out-of-phase

Fig. 6 Modified Γ-plane for TYPE 304 stainless steel at 550°C.

Γ-plane) separated into in-phase and out-of-phase shown in Fig. 6. In general, the contours can be expressed by the following equation:

$$\left(\frac{\Delta\gamma_{max}}{g} \right)^j + \left(\frac{\Delta\varepsilon_n}{h} \right)^j = 1 \quad \ldots (1)$$

where g, h and j are the constants obtained experimentally,

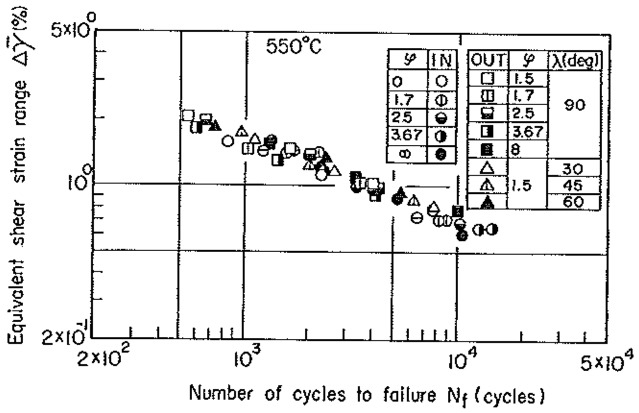

Fig. 7 Relationship between $\Delta\bar{\gamma}$ and fatigue failure life at 550°C.

which depend upon materials and temperature. From equation (1), the equivalent shear strain range, $\Delta\bar{\gamma}$, can be defined as follows;

$$(\Delta\bar{\gamma})^j = (\Delta\gamma_{max}/2)^j + A\Delta\varepsilon_n{}^j \quad \ldots\ldots\ldots\ldots\ldots\ldots\ldots (2)$$

where A is a constant which is experimentally determined. From the iso-Nf contours shown in Fig. 6, the value of j and A are found to be equal to 2 and 11.3 for in-phase, and 1 and 1.2 for out-of-phase. Therefore, $\Delta\bar{\gamma}$ for each phase is given by following formula;

$$\left.\begin{aligned} (\Delta\bar{\gamma})^2 &= (\Delta\gamma_{max}/2)^2 + 11.3\Delta\varepsilon_n{}^2 \quad \text{(In-phase)} \\ \Delta\bar{\gamma} &= \Delta\gamma_{max}/2 + 1.2\Delta\varepsilon_n \quad \text{(Out-of-phase)} \end{aligned}\right\} \ldots\ldots (3)$$

The relationship between the biaxial LCF life and the above criterion is shown in Fig. 7. This shows that very good correlation with $\Delta\bar{\gamma}$ can be obtained for all the test results, and it also confirms that $\Delta\bar{\gamma}$ is the valid criterion for predicting biaxial LCF life since it gives a comprehensive evaluation of Nf independent of the phase difference and the strain ratio. Fig. 8 shows the modified Γ-planes determined from the results obtained at R.T. and at 650°C. The solid and broken lines indicate the in-phase and out-of-phase iso-Nf contours, respectively. From these results, the $\Delta\bar{\gamma}$ is given as follows;

in the case of R.T.,

$$\left.\begin{aligned}(\Delta\bar{\gamma})^2 &= (\Delta\gamma_{max}/2)^2 + 21.2\Delta\varepsilon_n{}^2 \quad \text{(In-phase)}\\ \Delta\bar{\gamma} &= \Delta\gamma_{max}/2 + 1.7\Delta\varepsilon_n \quad \text{(Out-of-phase)}\end{aligned}\right\}\cdots\cdots\cdots \quad (4)$$

in the case of 650°C,

$$\left.\begin{aligned}(\Delta\bar{\gamma})^2 &= (\Delta\gamma_{max}/2)^2 + 12.0\Delta\varepsilon_n{}^2 \quad \text{(In-phase)}\\ \Delta\bar{\gamma} &= \Delta\gamma_{max}/2 + 1.2\Delta\varepsilon_n \quad \text{(Out-of-phase)}\end{aligned}\right\}\cdots\cdots\cdots \quad (5)$$

The correlation of biaxial LCF life at R.T. and at 650°C with $\Delta\bar{\gamma}$ is shown in Fig. 9. At both temperatures, fatigue life can be correlated well with $\Delta\bar{\gamma}$ regardless of the strain ratio and the phase difference. The experimental constants at these temperature are summarized in Table 3. The iso-Nf contours for the 650°C data are almost the same as those for the 550°C data so that the values of their experimental constants are nearly equal between them. At elevated temperatures, therefore, the following value of experimental constants, j and A, can be adopted; j=2 and A=1.20 for in-phase conditions and j=1 and A=1.2 for our-of-phase conditions. At R.T., the value of j is also 2 which is equal to the value at elevated temperatures. Since biaxial LCF data at R.T. are less than those at 550°C, the

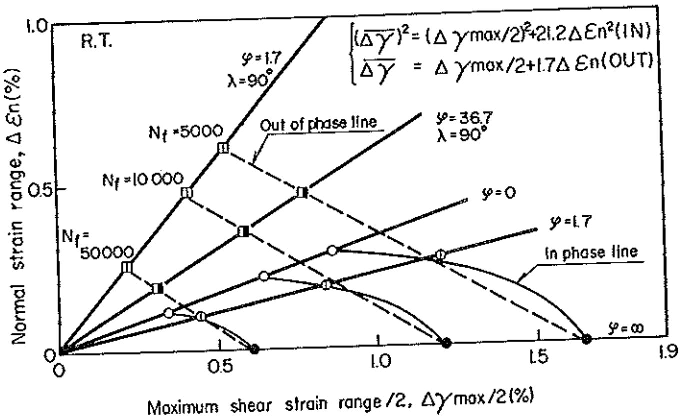

(a) R.T.

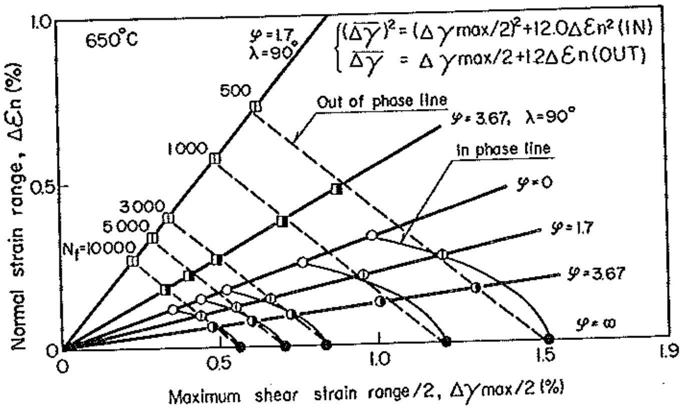

(b) 650°C

Fig. 8 Modified Γ-plane for TYPE 304 stainless steel at R.T. and 650°C.

Table 3 Material constants

Temp.	J		A	
	IN	OUT	IN	OUT
R.T.	2	1	21.2	1.7
550°C	2	1	11.3	1.2
650°C	2	1	12.0	1.2

value of A has not yet be fixed. However, the value of A under in-phase conditions could be determined from both uniaxial and torsional LCF data.

In order to discuss the validity of the equivalent shear strain criterion, the tension-torsion data obtained for 304 stainless steel by other researchers (2, 10, 16) were applied to correlate with $\Delta\bar{\gamma}$. The data are as follows; the data obtained under only in-phase condition at R.T. by Blass and Zamrik (2), and the data obtained under in-phase and out-of-phase conditions at R.T. by Socie (10). They were correlated with $\Delta\bar{\gamma}$ as defined in equation (4). The data of Sakane et al. (16) under only in-phase condition were also correlated with $\Delta\bar{\gamma}$ as defined in equation (5). The relationships are shown in Fig. 10. The tendency for biaxial LCF life to depend on the strain ratio is rarely seen in all of them, although such tendency was found in the case of the application of the classical criteria. It is, therefore, concluded that $\Delta\bar{\gamma}$ is the effective criterion.

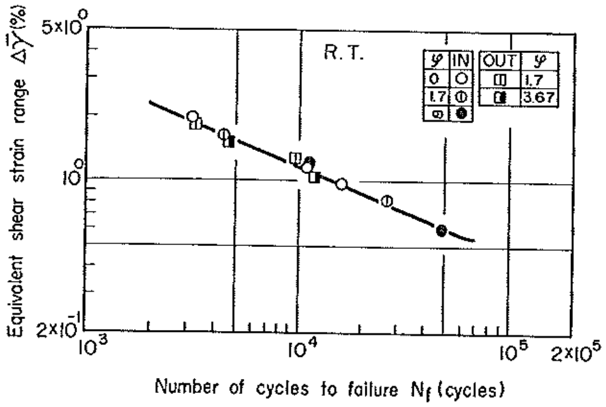

(a) R.T.

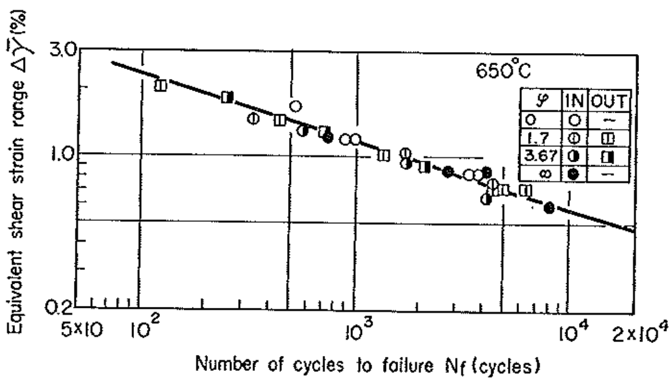

(b) 650°C

Fig. 9 Relationship between $\Delta\bar{\gamma}$ and fatigue failure life at R.T. and 650°C.

A mean stress effect is one of the problems in the biaxial LCF evaluation. Socie et al. (17) have investigated the mean stress and strain effect on biaxial LCF life of IN 718, and

Fatemi and Kurath (18) have also investigated the effect by using IN 718 and 1045 steel. Both the two research groups have reported that mean stress effect in significant if the mean stress does not relax, but not detrimental if the mean stress relaxes quickly enough to a significant amount. The mean stress and strain effect on fatigue life is not clear under biaxial LCF of TYPE 304 stainless steel since the data have not yet been available for discussing the mean stress and strain effects. More experimental studies are required to examine the mean stress and strain effect on biaxial the LCF life of TYPE 304 stainless steel.

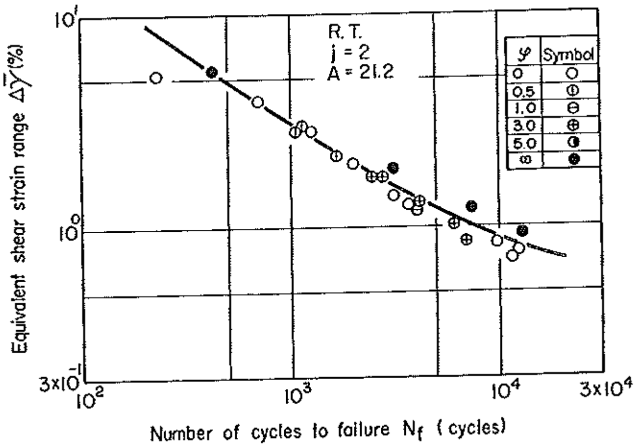

(a) R.T. (Blass and Zamrik)

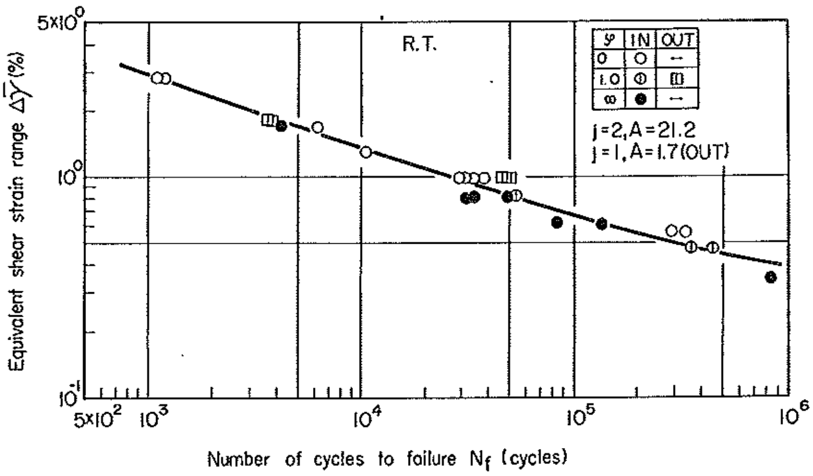

(b) R.T. (Socie)

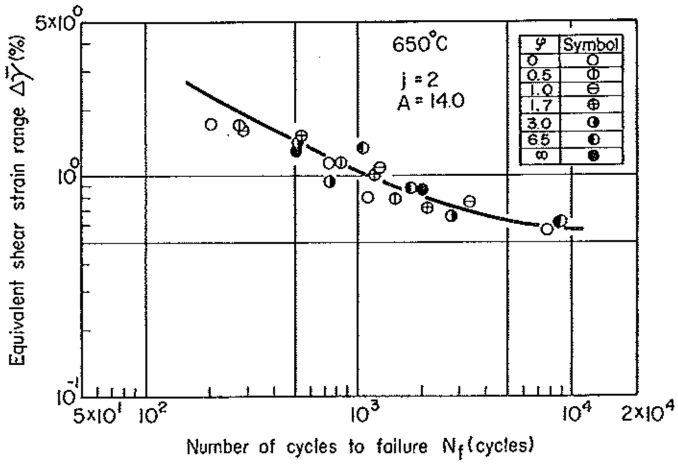

(c) 650°C (Sakane et al.)

Fig. 10 Correlation of biaxial LCF data with $\Delta\bar{\gamma}$

CONCLUSIONS

Axial-torsional strain-controlled fatigue tests on Type 304 stainless steel were conducted under in-phase and out-of-phase straining conditions at room temperature and 650°C. The results obtained can be summarized as follows.

1. The Mode II fractures occured only in pure torsion ($\Delta\gamma$= 1.21%) at 650°C due to the linking of microcracks initiating in a direction normal to the ε_1 direction on oxide layer. Under the other in-phase test conditions, the macrocracks propagated in the Mode I independent of the applied strain range. Under out-of-phase conditions, at both temperatures, the main cracks propagated in the circumferential direction, and fracture surfaces indicated that the main crack propagated under a mixed mode combining Modes I and II.

2. Although biaxial LCF data at both temperatures could not be correlated with the classical criteria, these data were correlated well with $\Delta\bar{\gamma}$, which was determined from the modified Γ-plane, regardless of the strain ratio and phase difference. The value of an experimental constant, j, in the criterion found to be 2 at both room and elevated temperatures.

3. The good relationships between $\Delta\bar{\gamma}$ and axial-torsional LCF life were also obtained by using the data reported by other researchers, and this confirmed that the $\Delta\bar{\gamma}$ in this study was applicable as a biaxial LCF failure criterion.

REFERENCE

1. Parsons M.W. and Pascoe K.J. (1975) Low cycle fatigue under biaxial stress. Proc. Instn. Mech. Engr. 188, 61-74

2. Blass J.J. and Zamrik S.Y. (1976) Multiaxial low-cycle fatigue of type 304 stainless steel. ASTM-MPC Symp. Creep Fatigue Interaction, 129-159

3. Brown M.W. and Miller K.J. (1979) High temperature low cycle biaxial fatigue of two steels. Fatigue Engng. Mater. Struct. 1, 217-229

4. Brown M.W. and Miller K.J. (1973) A theory for fatigue failure under multiaxial stress-strain conditions. Proc. Instn. Mech. Engr. 187, 745-755

5. Garud Y.S. (1979) A new approach to the evaluation of fatigue under multiaxial loadings. Trans ASME J. Engng. Mater. Technol. 103, 118-125

6. Lohr R.D. and Ellison E.G. (1980) A symple theory for low cycle multiaxial fatigue. Fatigue Engng. Mater. Struct. 3, 1-17

7. Hamada N. Sakane M. and Ohnami M. (1984) A study for high-temperature biaxial low-cycle fatigue failure criterion. Japan Society of Mechanical Engineers. A-50, 1838-1844 (in Japanese)

8. Konter A.W.A. Jassen G.T.M. and Husslage W. (1979) Effect of biaxial loading and geometry on prediction of low-cycle fatigue life. International conference on Structure Mechanics in Reactor Technology, Div. L, 13/1

9. Kandil F.A., Brown M.W. and Miller K.J. (1982) Biaxial low-cycle fatigue failure of 316 stainless steel at elevated temperature. Proc. Int. Conf. on Mech. Behav. Nucl. Appl. Stainless Steel at Elevated Temperature, 203-209

10. Socie D. (1987) Multiaxial fatigue damage models. Trans. ASME J. Engng. Mater. Technol. 108, 293-298

11. Kanazawa K., Miller K.J. and Brown M.W. (1979) Low-cycle fatigue under out-of-phase loading conditions. Trans. ASME J. Engng. Mater. Technol. 99, 222-228

12. Jordan E.H., Brown M.W. and Miller K.J. (1985) Fatigue under severe nonproportional loading. International Symposium on Biaxial/Multiaxial Fatigue, ASTM STP 853, 569-585

13. Ohnami M., Sakane M. and Hamada N. (1985) Effect of changing principal stress axes on low-cycle fatigue life in various strain wave shapes at elevated temperature. International Symposium on Biaxial/Multiaxial Fatigue, ASTM STP 853, 622-634

14. Kuwabara K., Nitta A. and Ogata T. (1987) The effect of straining phase on biaxial fatigue life at 550°C in type 304 stainless steel. Mechanical Behaviour of Materials (ICM-5), Vol. 2, 1173-1180

15. Nitta A. Ogata T. and Kuwabara K. Fracture mechanism and life assessment under high-strain biaxial cyclic loading in type 304 stainless steel. Fatigue Fract. Engng. Mater. Struct. To be published

16. Sakane M.,Ohnami M. and Sawada M. (1987) Fractue modes and low cycle biaxial fatigue life at elevated temperature. Trans. ASME J. Engng. Mater. Technol. 109, 236-243

17. Socie D.F., Waill L.A. and Dittmer D.F. (1985) Biaxial fatigue of Inconel 718 including mean stress effects. International Symposium on Biaxial/Multiaxial Fatigue, ASTM STP 853, 463-478

18. Fatemi A. and Kurath P. (1988) Multiaxial fatigue life predictions under the influence of mean-stresses. Trans. ASME J. Engng Mater. Technol. 110, 380-388